Heliyon 5 (2019) e02289

Contents lists available at ScienceDirect

Heliyon

journal homepage: www.heliyon.com

Heliyon

Cyclic β-(1, 2)-glucan blended poly DL lactic co glycolic acid (PLGA 10:90) nanoparticles for drug delivery

Geetha Venkatachalam, Nandakumar Venkatesan, Ganesan Suresh, Mukesh Doble *

Bioengineering and Drug Design Lab, Department of Biotechnology, IIT-Madras, Chennai, 600036, India

ARTICLE INFO

Keywords:
Materials science
Polymers
Biomedical engineering
Cyclic β-(1, 2)-glucan
PLGA
Blends
Drug delivery
Gentamicin

ABSTRACT

Our group had previously reported the encapsulation efficiency of cyclic β-(1, 2)-glucan for various drugs. The current study is aimed at evaluating the use of glucan as a drug carrier system by blending with poly lactic-co-glycolic acid (L:G = 10:90). Nanoparticles of glucan (0.5, 5, 10 and 20 wt %) blended with PLGA and gentamicin were synthesized. Encapsulation efficiency was higher for the blends (93% with 20 wt % of glucan) than the PLGA alone (79.8%). The presence of glucan enhanced both the biodegradability, and biocompatibility of PLGA. Degradation of the nanoparticles *in vitro,* was autocatalytic with an initial burst release of active drug and the release profile was modeled using the Korsmeyer-Peppas scheme. *In vivo* studies indicated that the drug released from the blends had high volume of distribution, and greater clearance from the system. Pharmacokinetics of the drug was predicted using a double exponential decay model. Blending with PLGA improved the drug release characteristics of the cyclic β-(1, 2)-glucan.

1. Introduction

Cyclic β-(1,2)-glucans (CβG) are water soluble, biocompatible, and biodegradable, extracellular polysaccharides produced by *Rhizobiaceae* and *Agrobacteriaceae* family [1, 2, 3]. They help the bacterium in osmoregulation, and during plant infection [4, 5, 6, 7]. The molecular weight of these polymers, ranges between 1 to 6 kDa, with the degree of polymerization from 14 to 28. Each ring size of the CβG exists as a mixture of conformations that have cavities of variable size and polarity [8, 9, 10, 11]. As a result, they form inclusion complexes with both polar and nonpolar compounds including poorly water-soluble molecules such as mefenamic acid, vitamins, phenylbutazone, indomethacin, steroids, paclitaxel, vitamins, ergosterol, amphotericin B, flurbiprofen, luteolin and betulinic acid [8, 9]. CβG had been reported to have good encapsulation efficiency for various drugs (with 85–99 % efficiency) including dexamethasone, umbelliferone, curcumin, 6-methylcoumarin, 4-hydroxycoumarin and 4 methyl umbelliferone [12]. Since the glucans are completely water soluble, the encapsulated drugs exhibit initial burst release which depends on the specificity of drug and the binding constant. In order to control the initial burst release, and prolong the release of drug, we propose to blend CβG with a synthetic polymer (PLGA).

Synthetic poly DL lactic co glycolic acid (PLGA), copolymers of lactic acid and glycolic acid, is widely used and tested as a carrier molecule for the delivery of proteins, peptides, drugs, DNA and RNA [13]. PLGA was blended with pluronic (poly (ethylene oxide) (PEO), polypropylene oxide (PPO) or poly (ethylene oxide) (PEO) triblock co polymer to achieve sustained drug release (paclitaxel) [14, 15]. Nanoparticles of copolymer monomethoxy (polyethylene glycol)-poly (D, L lactide-co-glycolide) - poly (L-lysine) were tested for targeted drug delivery of adriamycin (anti-cancer drug) and siRNA (small interfering RNA-negative) in tumor cells [16]. Fab-conjugated nanoparticles of PLGA were developed to effectively target cancer cells expressing CD44v6 [17]. Among different polymers tested, PLGA10:90 (molar ratio of lactic acid 10, glycolic acid 90) was reported to have better encapsulation efficiency and sustained drug release for hydrophilic drug meropenem than the higher lactic acid polymers [18].

In the present study, CβG was blended with PLGA (10:90) and polyvinyl alcohol (PVA) to improve the drug release characteristics of CβG. PVA is a hydrophilic polymer and it has been used as a surfactant to form nanoparticles of uniform size [19].

2. Materials and methods

Gentamicin (Abbott, India), PVA (Sigma Aldrich, India), *Escherichia coli (E.coli)* (National Collection of Industrial Microorganisms (NCIM),

* Corresponding author.
E-mail address: mukeshd@iitm.ac.in (M. Doble).

https://doi.org/10.1016/j.heliyon.2019.e02289
Received 6 January 2019; Received in revised form 12 April 2019; Accepted 8 August 2019

Pune), L6 myoblast cells (National Centre for Cell Science (NCCS), Pune, India), Dulbecco's modified Eagle's medium (Himedia, India), Fetal bovine serum (Gibco, India). All other chemicals used were of analytical grade. *In vivo* experiment was carried out in C. L. Baid Metha College of Pharmacy, Chennai, India. Animal use and the experimental protocols were approved by the institutional animal ethics committee (IAEC).

2.1. Preparation of CβG and PLGA (L:G = 10:90) polymer synthesis

CβG was produced from *Rhizobium meliloti* (MTCC 3402) in mannitol glutamic acid medium [5], and the extracellular glucan was extracted by ethanol precipitation, and purified using Biogel P6 (Biorad, USA). Glucan was completely water soluble (solubility: 250 gm/L). The molar mass of Cβg was 3101.46 Da (with DP size of 17–28) [20]. PLGA (10:90) (87 kDa) used in the current study was synthesized by direct melt condensation process with $SnCl_2$ as a catalyst at 160 °C [21].

2.2. Gentamicin loaded CβG/PLGA nanoparticle synthesis

Blends of CβG and PLGA was prepared by mixing the polymers in four different weight ratios (wt %). P1 (PLGA– 100%), P2 (0.5% CβG with 99.5 % PLGA), P3 (5 % CβG with 95 % PLGA), P4 (10 % CβG with 90 % PLGA) and P5 (20 % CβG with 80 % PLGA). Nanoparticles of CβG-PLGA blends with and without the drug was prepared by the emulsion solvent evaporation method [22]. Solutions of varying concentrations of PLGA (100, 99.5, 95, 90, 80 % w/v) in tetrahydrofuran (THF) (with 0.25% trifluoro acetic acid (TFA)) were prepared. Varying quantities of glucan (0.5, 5.0, 10 and 20 % w/v) were solubilized in water. Respective solutions were mixed together and sonicated (30 % amplitude) for 60 min. Aqueous solution of gentamicin (800 mg/ml) was added to this mixture. The mixture was then added drop wise to 0.3 % polyvinyl alcohol solution (100 ml) and homogenized for 30 min using a microtip probe sonicator (Sonics & Materials Inc., USA). Partial vacuum was applied to remove the organic phase and the remaining solution was centrifuged at 12,000 rpm for 20 min. Pellet containing gentamicin loaded nanoparticles was lyophilized and used for further analysis.

2.3. In vitro drug release from the nanoparticles

10 mg of gentamicin loaded nanoparticles was suspended in phosphate buffer saline (5 ml, pH 7.2) in a falcon tube and kept under continuous shaking (120 rpm) at 37 °C. At different time intervals the tubes were centrifuged at 12,000 rpm for 20 min and the supernatant was collected. The nanoparticles were resuspended in fresh PBS and left in the shaker. Supernatant was filtered with 0.45 μm membrane filter and the absorbance was measured at 330 nm with a UV-visible spectrophotometer (Jasco V-550, Japan) [18, 23] with pure gentamicin as standard.

2.4. Characterization of the nanoparticles

Size distribution of the nanoparticles was determined by Zetatrac Particle size analyzer (Microtrac Inc., USA) at 780 nm with a back-scattering angle of 180°. 1 mg/ml of drug loaded polymeric nanoparticles was suspended in distilled water to reach a final concentration of 100 μg/ml and used for the analysis. Morphology of the nanoparticles was visualized under a transmission electron microscope (Philips/FeiCM-20). Nanoparticles (P1–P5) were mixed with KBr pellets (at a ratio of 1:20) and the infra-red spectrum was recorded from 4000–400 cm^{-1} with Perkin-Elmer PE1600 FTIR spectrometer. Thermal stability of the nanoparticles was determined by differential scanning calorimeter (Netzsch DSC 204) and thermo gravimetric analyzer (TGA Q500V20.10 Universal TA instrument) in a nitrogen atmosphere from 10 to 140 °C and 30–930 °C respectively at a heating rate of 10 °C/min. ^{1}H NMR (Nuclear magnetic resonance spectroscopy) spectrum of the material was measured (Bruker 500 MHz spectrometer) with 10 mg of sample dissolved in D_2O and a drop of TFA. Molecular weight of the polymer was determined by using gel permeation chromatography with tetrahydrofuran as the mobile phase (flow rate of 1 mL/min at 35 °C), and polystyrene (Easical, Polymer laboratories, UK) as internal standard.

2.5. Antimicrobial activity of released gentamicin

Activity of the released drug was determined by a method reported earlier with some modifications [24]. 10 mg of gentamicin loaded nanoparticles were suspended in phosphate buffer saline (5 ml, pH 7.2) in a falcon tube and kept under continuous shaking at 120 rpm and 37 °C. At different time intervals the tubes were centrifuged at 12,000 rpm for 20 min and the supernatant was collected and lyophilized. Cultures of *E. coli* NCIM 2931 prepared in Luria broth (OD of 0.005) was added to a 96 well clear bottom plate and the drug released from the nanoparticle was added to the each well and incubated at 37 °C for 24 h. The percentage inhibition of bacterial growth was calculated by the using the formula below, with pure gentamicin as positive control.

$$\%\ \text{Growth inhibition} = 100 \times \left[OD_{test} / OD_{positive\ control}\right]$$

2.6. Biocompatibility of nanoparticles

L6 myoblast cells were cultured in DMEM (Medium contains DMEM with 10% FBS and 1% of 100 X antibiotic-antimycotic liquid) in a CO_2 incubator (Astec, Japan) (temperature 37 °C, carbon dioxide level 5 %). Approximately10^4 cells were seeded into a 96 well polystyrene plate and incubated for 24 h. The cells were then incubated with 500 μg/ml of CβG/PLGA nanoparticles for another 24 h. Total number of viable cells was determined by MTT (3-(4, 5- Dimethylthiazol-2-yl)-2, 5-diphenyltetrazolium bromide) based cell proliferation assay [25].

2.7. In vivo gentamicin release

2.7.1. Experimental animals

Adult male Wistar rats weighing 220–240 g were used in the present study. The inbred animals were procured from the animal house of C.L. Baid Metha College of Pharmacy, (Thoraipakkam, Chennai, India) and were housed six per cage under standard laboratory conditions at room temperature (22 ± 2 °C) with 12 hr light/dark cycle. The animals were provided with standard pellet chow and water ad libidum. Animals were acclimatized to laboratory conditions one week prior to initiation of experiments.

2.7.2. Tail vein injection

Rats were placed in a tail flick cage with the tail part outside; tail vein was identified by applying the nominal pressure on the surface. IV infusion set was inserted into the tail vein and kept undisturbed. Syringe containing the drug solution was connected with the infusion set up and the drug solution was slowly infused in to the tail vein for about 30 s.

Wistar rats were divided into four groups with 6 animals in each; group I rats were injected with 2 mg of pure gentamicin by intravenous infusion and group II to IV rats were injected with 10 mg of gentamicin encapsulated CβG/PLGA nanoparticles which contain approximately ~4 mg of the drug.

2.7.3. Detection of concentration of released gentamicin

Blood samples (500 μl) were collected at 0.5, 1, 1.5, 2, 2.5, 3, 3.5, 4, 4.5, 5, 6, 8, 24, 48 and 72 h after injection by retro-orbital plexus puncture technique [26]. The plasma was separated from the blood by centrifugation at 3500 rpm for 10 min. 100 μl of plasma was added to 200 μl of phosphate buffer saline, vortexed and centrifuged at 3500 rpm for 3 min. 20 μl of the sample was injected into HPLC (5 μm C18 reverse phase

analytical column with mobile phase consisting of 0.2 M of Na_2SO, 0.02 M of sodium pentane sulfonate and 0.1 % (v/v) of acetic acid in water – methanol (97:3) at a pH of 3.4). The peaks were monitored using a UV detector at a wavelength of 300–330 nm. The amount of drug in the blood plasma was determined from the standard graph, with pure gentamicin as standard [27].

3. Results and discussion

3.1. Characterization of gentamicin loaded CβG/PLGA nanoparticles

Presence of characteristic functional groups of CβG and PLGA in the blend was confirmed by FTIR spectroscopy. The peak at 3513 cm^{-1} corresponds to the OH, 2992 and 2960 cm^{-1} corresponds to the CH stretching, 1628 cm^{-1} corresponds to amide bond, and 1093 cm^{-1} corresponds to the CN peak of gentamicin [28]. PLGA has characteristic bands corresponding to CH (2637 cm^{-1}), and carbonyl (1745 cm^{-1}). The peaks corresponding to hydroxyl (3503 cm^{-1}) and C–C–O stretch (1086 cm^{-1}) indicates the presence of CβG. These characteristic peaks were observed in all the four ratios (P2–P5) (Figs. S1–S5 Supporting information). The IR spectra of all the blends confirmed the presence of both the polymers in the blend. The presence of drug in the polymer nanoparticles were confirmed from the –CN stretch of gentamicin.

Table 1
^{1}H NMR Chemical shift values and FTIR spectra wavenumbers of CβG/PLGA nanoparticles.

Name of the Polymer	^{1}H NMR	FTIR
P1	8.69 (s, 1H), 8.41 (s, 3H), 6.842–6.41 (m), 5.54 (d, J = 10Hz), 5.32–5.24 (m), 5.12 (s), 5.042–5.02 (m), 4.97(s), 4.94–4.84 (m), 4.69 (s), 4.62–4.55 (m) 4.49–4.39 (m), 2.91 (s), 2.37 (d), 2.34 (s), 2.21 (s), 2.02–2.00 (m), 1.82 (d, J = 5Hz), 1.74 (s), 1.72 (s), 1.652–1.58 (m), 1.372–1.28 (m), 0.90 (s)	OH (3513 cm^{-1}), CH (2992 cm^{-1}), CH (2960 cm^{-1}), CH (2637 cm^{-1}), carbonyl (1745 cm^{-1}), amide (1628 cm^{-1}), CO peak (1171 cm^{-1}), CN peak (1093 cm^{-1}).
P2	8.85 (s), 8.64 (s), 6.82–6.39 (m), 5.54 (d, J = 5Hz), 5.32–5.24 (m), 5.12 (s), 5.03–5.02 (m), 4.98 (s), 4.94–4.84 (m), 4.68 (s), 4.49–4.48 (m), 4.44 (s), 4.01 (s), 3.97 (t, J = 10 Hz), 3.75 (s), 3.59 (s), 2.91 (s), 2.47 (t, J = 10Hz) 2,34 (s), 2.22 (s), 2.18 (s), 2.02 (t), 1.82 (d, J = 5 Hz), 1.742–1.59 (m), 1.33–1.22 (m), 0.90 (s)	OH (3513 cm^{-1}), CH (2992 cm^{-1}), CH (2960 cm^{-1}), CH (2637 cm^{-1}), carbonyl (1745 cm^{-1}), amide (1629 cm^{-1}), CO peak (1171 cm^{-1}), CN peak (1094 cm^{-1}), glycosidic bond (1000-1100 cm^{-1})
P3	10.03 (s), 6.61 (t), 5.36–5.31 (m), 5.05–4.83 (m), 4.54–4.36 (m), 4.02 (s), 3.97 (s), 3.79 (s), 3.62 (s), 2.54 (t), 2.35 (s), 2.22 (s), 2.02 (t), 1.742–1.55 (m), 1.38–1.30 (m), 0.92 (t)	OH (3513 cm^{-1}), CH (2992 cm^{-1}), CH (2960 cm^{-1}), CH (2637 cm^{-1}), carbonyl (1745 cm^{-1}), CO peak (1171 cm^{-1}), CN peak (1093 cm^{-1}), glycosidic bond (1000-1100 cm^{-1})
P4	9.86 (s), 6.61 (t), 5.62 (s), 5.34 (s), 5.04–4.87 (m), 4.50–4.38 (m), 4.02 (s), 3.97 (s), 3.78 (s), 3.58 (s), 2.35 (s), 2.02 (s), 1.70 (s), 1.63 (s), 1.29 (s), 0.90 (s)	OH (3513 cm^{-1}), CH (2992 cm^{-1}), CH (2960 cm^{-1}), CH (2637 cm^{-1}), carbonyl (1745 cm^{-1}), amide (1624 cm^{-1}), CO peak (1171 cm^{-1}), CN peak (1093 cm^{-1}), glycosidic bond (1000-1100 cm^{-1})
P5	9.34 (s), 9.09 (s), 6.84–6.34 (m), 5.37–5.30 (m), 5.08–4.83 (m), 4.50 (d), 3.96 (s), 2.38 (d), 2.21 (s), 2.01 (s), 1.78 (d), 1.62 (d), 1.29 (s), 0.90 (s)	OH (3513 cm^{-1}), CH (2992 cm^{-1}), CH (2960 cm^{-1}), CH (2637 cm^{-1}), carbonyl (1745 cm^{-1}), amide (1624 cm^{-1}), CO peak (1171 cm^{-1}), CN peak (1093 cm^{-1}), glycosidic bond (1000-1100 cm^{-1})

The presence of both the polymer and drug was also confirmed by proton NMR spectra. The peaks were consistent with the earlier reported data for CβG and PLGA (10:90) [12, 21]. Further, the presence of both polymers in the different blends were confirmed by their ^{1}H NMR spectra (Figs. S6–S10 Supporting information). The chemical shift values corresponding to CβG/PLGA drug nanoparticles are listed in Table 1. The chemical shift values δ 8.69 (s, 1H) and 8.41 (s, 3H) indicate the presence of PLGA in P1, upon increasing the concentration of glucan these two PLGA peaks merged into a single peak (P2–P5). δ 5.12 (s) is the amine peak of gentamicin, and 2.91 (s) is the OH peak of gentamicin. In the blends P2 to P5, chemical shift values of CβG δ 3.79 (dd J_1 = 5Hz, J_2 = 5Hz), 3.72 (s), 3.70 (s), 3.40 (s), 3.57, 3.68, 3.60 (q), 3.44 (d), and 4.78 (m) and that of gentamicin 2.47 (t) were merged with that of the PLGA peaks (Fig. 1). The weight average molecular weight of the PLGA was 87 kDa. The TGA spectrum (Fig. 2) showed maximum weight loss at 300 °C (50 %). The melting temperature of P1 was 25.84 °C (data not included). Addition of CβG decreased the melting temperature of the blends (values for P2–P5 were 25.07, 24.06, 24.73 and 24.22 °C respectively). TGA of pure CβG indicated a maximum weight loss below 200 °C, whereas the blends (P2 to P5) showed maximum weight reduction at 300 °C.

The nanoparticles were spherical shaped (Fig. 3). These particles appeared as core-shell where the inner phase could be attributed to gentamicin loaded glucan and the outer phase to PLGA. Moreover, the phase separation was not evident, which necessitates further investigation of this blend.

Encapsulation efficiency of blends P1 – P5 (Table 2) showed that with the increasing CβG content in the blend, the percentage of drug encapsulated increased. The amount of drug per weight of nanoparticle (drug + polymer) also increased from 38 to 42 % respectively. It has been reported that PLGA (50:50) nanoparticles had poor encapsulation efficiency (11–58.2 %) for water soluble drugs [29] but it was 67.35 % for paclitaxel [30] and 82 % for meropenem [18].

In vitro weight loss of the gentamicin loaded CβG/PLGA nanoparticles and its reduction in size as a function of time (Fig. 4A and B) showed a sharp decrease followed by a relatively slow decrease in size with time. The sudden decrease in weight of the nanoparticle as well as size could be attributed to the water solubility of CβG. The degradation of nanoparticles could be modelled as an autocatalytic reaction, because the degradation of PLGA released acid which in turn catalyzes and enhances this dissolution process further. So, the weight of the particles as a function of time could be represented as

$$W = Wo\beta e^{-\beta k_2 t} / \left[\beta - Wo + Woe^{-\beta k_2 t}\right] \quad (1)$$

$$\beta = [k_1 + k_2 Wo]/k_2$$

where

W and Wo - the weights of the nanoparticles at time - t and 0 respectively.
k1 and k2 - the rate constants corresponding to the following reactions respectively
A → B
A + B → 2B

B was assumed to be the degraded product which enhanced the degradation of the blend (A) further. Fig. 5 compares the experimental and model weight loss of the polymer as a function of time for P2 and P5 blends.

The corresponding k1 and k2 values obtained by fitting the data was 0.017 and 0.0115 for P2; 0.018 and 0.0139 for P5 respectively. As expected, increasing CβG content in the blend (from 5 % in P2 to 20 % in P5) increased the rates of reactions since it is highly soluble in water. The model fits the degradation data reasonably well. Autocatalytic degradation [13, 31] of the nanoparticle was also observed in the drug loaded PLGA nanoparticles which was successfully modeled.

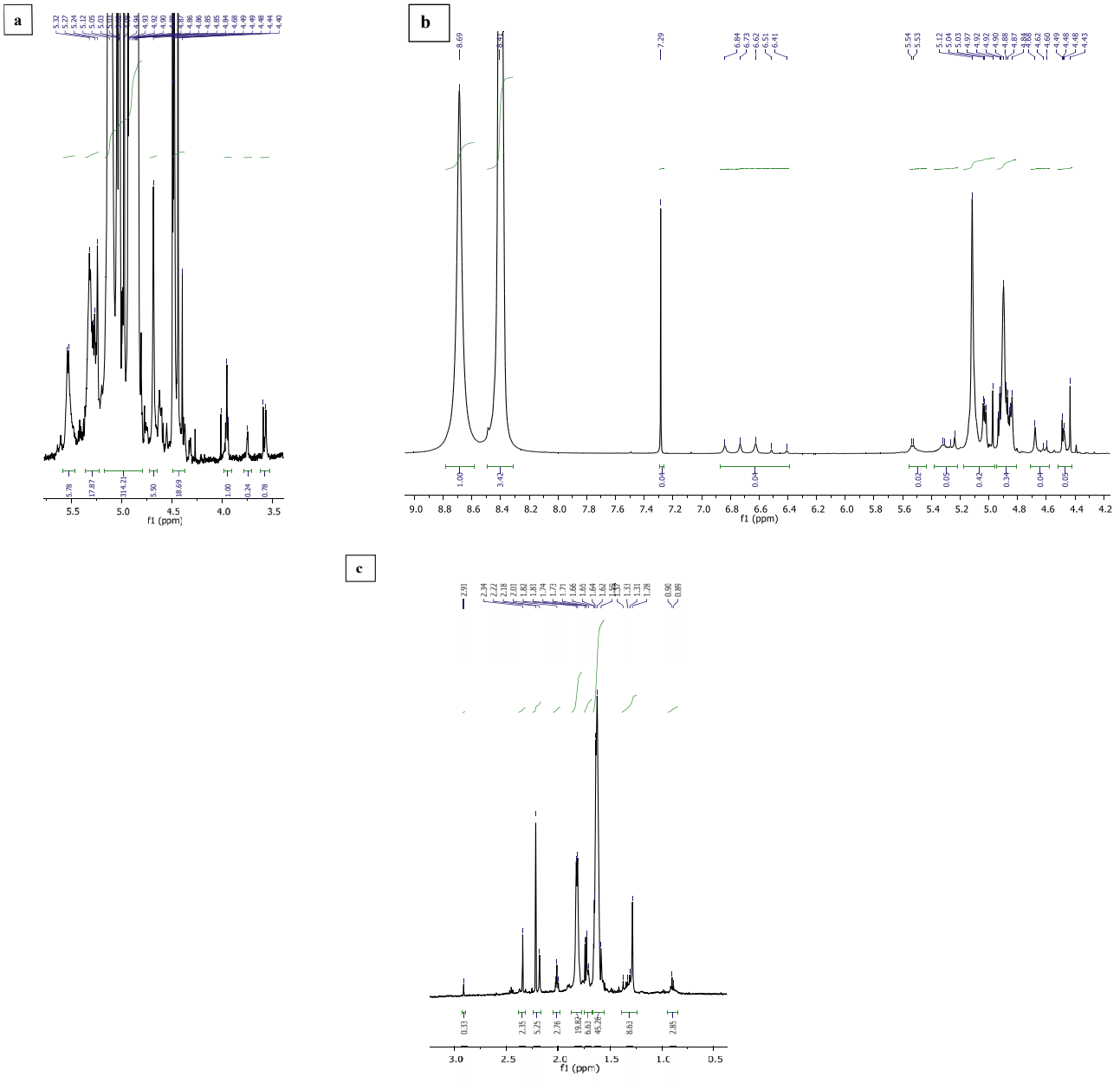

Fig. 1. Characteristic expansion ^{1}H NMR spectrum of a.) CβG, b.) PLGA, c.) Gentamicin from gentamicin loaded CβG/PLGA nanoparticles.

3.2. In vitro gentamicin release profile of CβG/PLGA (10:90) nanoparticles

The *in vitro* release of gentamicin from the nanoparticles for all the blends (Fig. 6A) showed an initial burst release and the rate of initial burst release was higher with glucan blended polymers (P2, P3, P4 and P5) than PLGA alone. After the initial burst release, sustained drug release was observed with all the blends. The percentage of drug released at the end of 37 days was higher with glucan-blended nanoparticles than PLGA alone. The higher drug release in the case of glucan blended nanoparticles could be attributed to higher encapsulation, and enhanced degradation rate of glucan by hydrolysis which was also in line with physical weight loss, and decrease in size of the nanoparticles. There exists a strong positive correlation between weight loss of the nanoparticles and drug release (correlation coefficient >0.92).

Drug release from the nanoparticles could be mathematically represented assuming Korsmeyer-Peppas model [32].

$$C_t = C_t K t^n \tag{2}$$

C_t and C_f- percentage of drug released at time = t and final equilibrium condition respectively, n - exponent.

Fig. 6B compares the experimental drug release and model predictions as a function of time for P2 and P5 blends. The corresponding KC_f and n values obtained by fitting the data was 0.308 and 0.245 for P2, and 0.395 and 0.22 for P5 respectively. As expected, increasing CβG content in the blend increased the drug release rate and a simple model fitted the drug release reasonably well. *In vitro* experiments on gentamicin and PLGA (at 50:50 weight ratio) microparticles showed 17–97 % encapsulation [33], whereas in our experiment, the particles showed 79–93 % in nano size (200 nm). Among the different synthetic polymers,

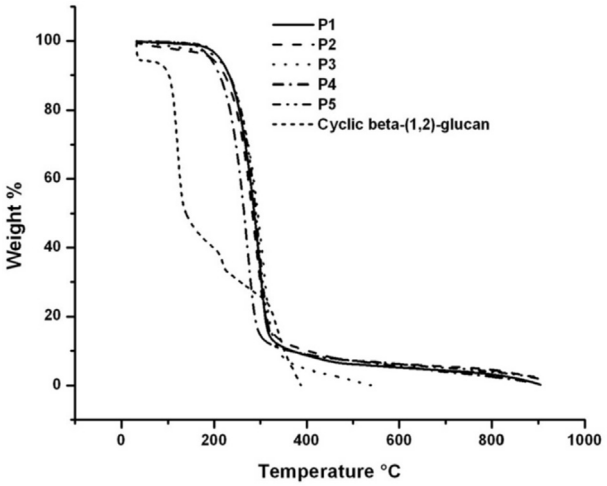

Fig. 2. Thermogravimetric analysis of the gentamicin loaded CβG/PLGA nanoparticles.

PLGA nanoparticles were well-known for their ability to associate and release molecules in a controlled manner [34, 35, 36]. In the current study, the P5 blend had high encapsulation (93 %). Several factors influence the release of the drug including its interaction with the polymer, polymer composition, size and geometry. Super paramagnetic iron oxide nanoparticles and dexamethasone acetate encapsulated by PLGA microparticles had complete release of the corticosteroid drug within a week, both *in vitro* and *in vivo* [37, 38]. In the current study the *in vitro* drug release was observed up to 37 days, because the polymer had a high molecular weight. PLGA nanoparticle (190–204 nm) with surface modification (human serum albumin) proved to be an ideal candidate for the delivery of anticancer drug [39].

3.3. Antimicrobial activity

The drug released from the nanoparticles inhibited the growth of *E. coli* (Fig. 7). The maximum inhibition was observed with P5 (~93.6 %) (within 1 h) and reached a plateau of 88 % inhibition and remains constant until day 37. These results indicate that P5 with 20 % glucan is a

Table 2
Encapsulation efficiency of various CβG/PLGA blends for gentamicin.

Name of the Polymer	Drug encapsulation (%)	Weight of drug (mg)/weight of nanoparticle (mg)
P1	79.80	0.38
P2	82.5	0.39
P3	85.7	0.40
P4	86.5	0.40
P5	93	0.42

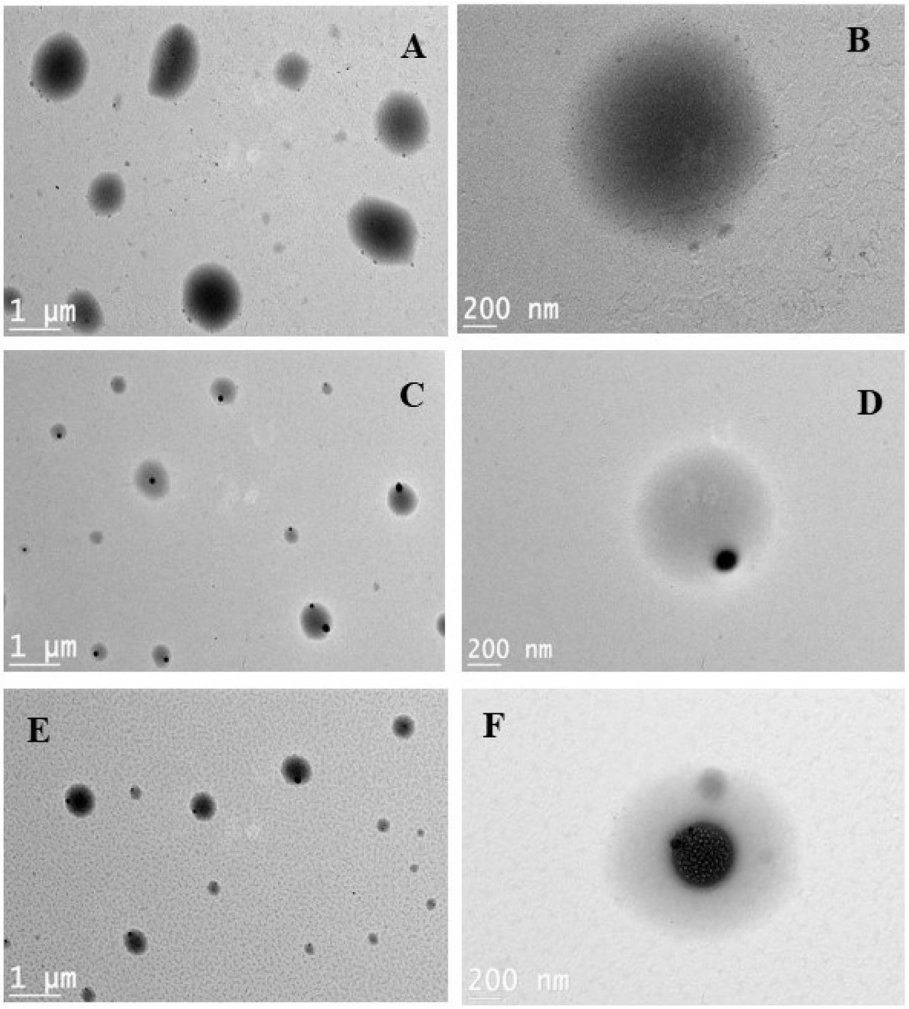

Fig. 3. Transmission electron microscopic images of drug loaded nanoparticles, P1 (A & B - PLGA 100%), P2 (C& D - CβG/PLGA = 0.5:99.5 %), P3 (E & F - 5 % CβG with 95 % PLGA). Nanoparticles appeared as core-shell where the inner phase could be attributed to gentamicin loaded glucan and the outer phase to PLGA.

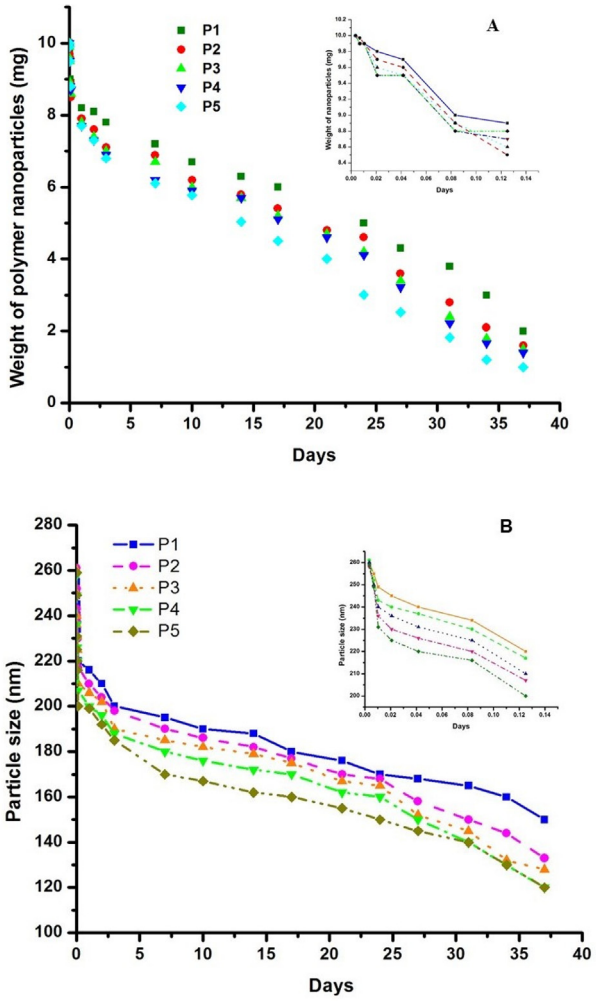

Fig. 4. Degradation of CβG/PLGA nanoparticles as a function of time (Inset - 5 h data). A. Weight of nanoparticles B. Nanoparticle size.

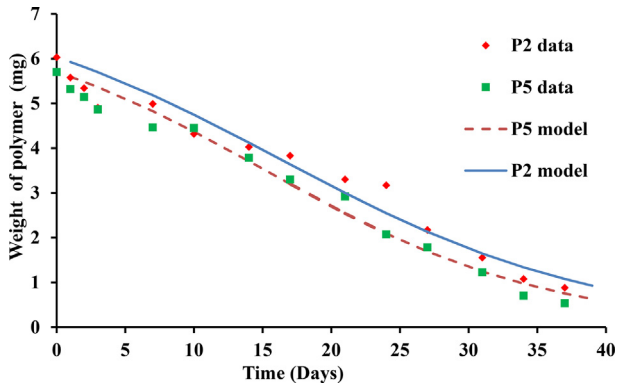

Fig. 5. Comparison of experimental and model predictions on the weight of the polymer.

better drug carrier than other blends.

The bacterial inhibition at the end of 37th day was high with P5 (85.7 %) followed by P3 (84 %) which could be attributed to the sustained release of drug. P1 showed the least inhibition at the end of 37th day.

3.4. Biocompatibility of PLGA and different ratios of CβG

Among the five different nanoparticles tested, P5 containing 20 % glucan was highly biocompatible against L6 myoblasts which could be attributed to the presence of high glucan content [12, 40]. CβG/PLGA nanoparticles were biocompatible towards L6 myoblast cells. With P1, 75 % cells were viable when treated with a concentration of 500 μg/ml whereas the viability was above 83 % with glucan blended nanoparticles (Fig. S11 Supporting information).

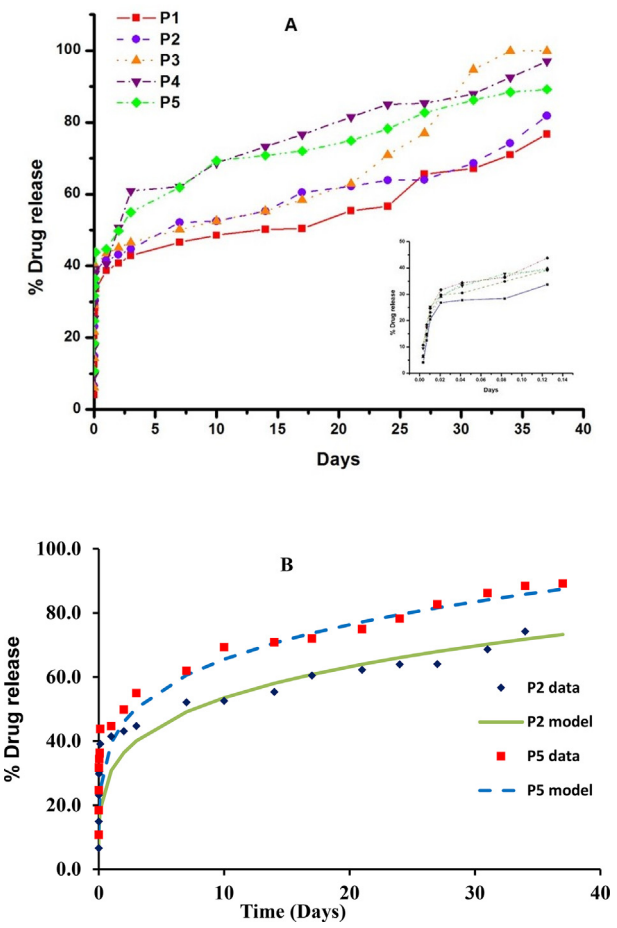

Fig. 6. *In vitro* gentamicin release from the CβG/PLGA nanoparticles. A. Experimental data (Inset - 5 h drug release). B. Model predictions for P2 & P5.

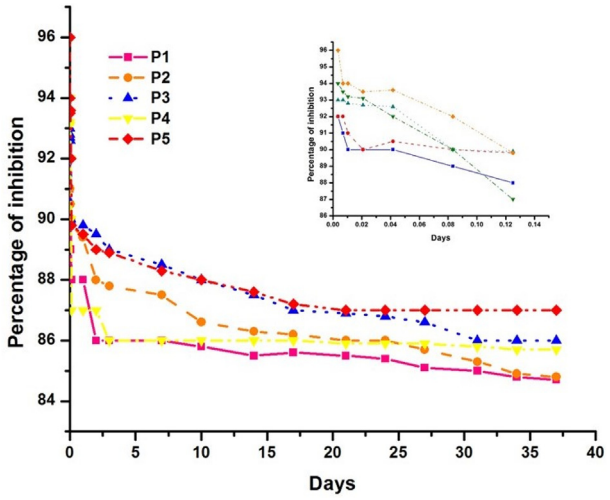

Fig. 7. Activity of gentamicin released against *E. coli in vitro* (Inset - 5 h *E. coli* inhibition).

3.5. *In vivo* drug release profile of CβG/PLGA nanoparticles

Group I rats were injected with pure gentamicin at a concentration of 2 mg/ml, whereas group II – IV were injected with 10 mg/ml of drug loaded nanoparticles (containing 3.8, 3.9 and 4 mg of pure drug in P1, P2 and P3 nanoparticles respectively). The *in vivo* results of three batches were included in supporting information Fig. S12.

Area under the curve (AUC) depends on the amount of drug administered and its rate of elimination [40]. There was no significant difference between the AUC of pure drug, and drug released from CβG-PLGA blends (Table 3), which indicated that the bioavailability of gentamicin in all cases were similar. Clearance which is a measure of amount of drug cleared from plasma in unit time [41], was high with (0.020 ml h^{-1} kg^{-1}) CβG-PLGA nanoparticles than the pure drug alone (0.005 ml h^{-1} kg^{-1}). Faster clearance rate was also reported for many anticancer drug delivery systems [26]. The reason for high clearance could be attributed to three different mechanisms including disintegration of the particle by binding to the proteins, clearance by the immune cells, and removal due to filtration by the cells [42]. Clearance also depends on the physico chemical properties of the drug. Faster clearance is very much essential for drugs such as gentamicin which is toxic to the nephrons [43] as it helps to reduce the side effects. Gentamicin was detectable in the plasma up to 6 h in the case of pure drug (Fig. 8), whereas it was detectable up to 8 h with PLGA (P1) alone and glucan blended PLGA (P2 & P3).

Volume of distribution (Vd), an apparent volume of blood plasma in the body in which the drug could be completely dissolved, was higher for blended nanoparticles than the pure drug. A value of Vd < 0.07 L/kg indicated that the drug was confined to the circulatory system and it was homogeneously distributed within the blood [44]. Prolonged drug release with similar AUC, high Vd, and clearance with the CβG-PLGA blends suggests that the blended nanoparticles could be ideal candidates for *in vivo* delivery of toxic drugs to achieve similar therapeutic effect of pure drug with better efficacy and safety. Similar results were also observed with paclitaxel, loaded PLGA 50:50 nanoparticles for long term treatment of breast cancer [26].

From Fig. 8 it was clear that the *in vitro* and *in vivo* gentamicin release were different. This could be due to the differences in the solubility, and degradation pattern of the polymers in PBS and blood plasma. So, the gentamicin concentration (C (t)) in the blood plasma was mathematically modeled with two exponential terms, one for the drug released from the particles into the blood stream (ka) and the other for its elimination (ke) from the body. Both the processes were assumed to be first order, resulting in the following relationship

$$C(t) = A\left[e^{-k_e t} - e^{-k_a t}\right] \quad (3)$$

Fig. 9 (A and B) compares the model predictions and the actual values for two different cases (P1 and P2). As seen, the model predicted the slow rise in the concentration and exponential fall, well. The values of A, k_a and k_e for P1 were 1300 μg/ml, 0.75 hr^{-1}, and 0.742 hr^{-1} respectively and for P2 it was 1350 μg/ml, 0.75 hr^{-1}, and 0.742 hr^{-1} respectively. The dotted line in Fig. 9A shows the prediction based on the burst release model (Korsmeyer-Peppas model) and could be seen this model predicts fast drug release from the nanoparticles unlike what is observed here.

Table 3
In vivo pharmacokinetic parameters of pure gentamicin and gentamicin released from CβG/PLGA nanoparticles.

Pharmacokinetic parameters	Pure drug	PLGA (P1)	CβG: PLGA (P2)	CβG: PLGA (P3)
$AUC_{0-\infty}$ (μg h/ml)	203	196	201	200
Clearance (ml h^{-1} kg^{-1})	0.005	0.020	0.020	0.020
Volume of distribution (ml/kg)	0.1	0.6	0.6	0.6
C_{max} (μg/ml)	8.4	5.3	6.2	7.2
T_{max}(h)	1.0	1.5	1.0	2.0

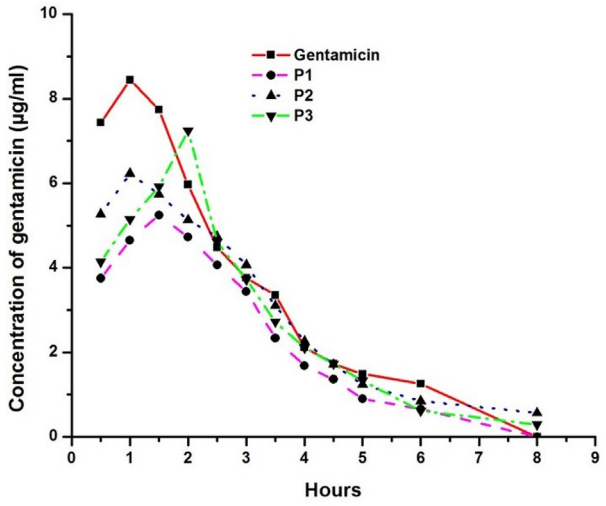

Fig. 8. *In vivo* plasma concentration of gentamicin released from the CßG/PLGA nanoparticles and pure gentamicin.

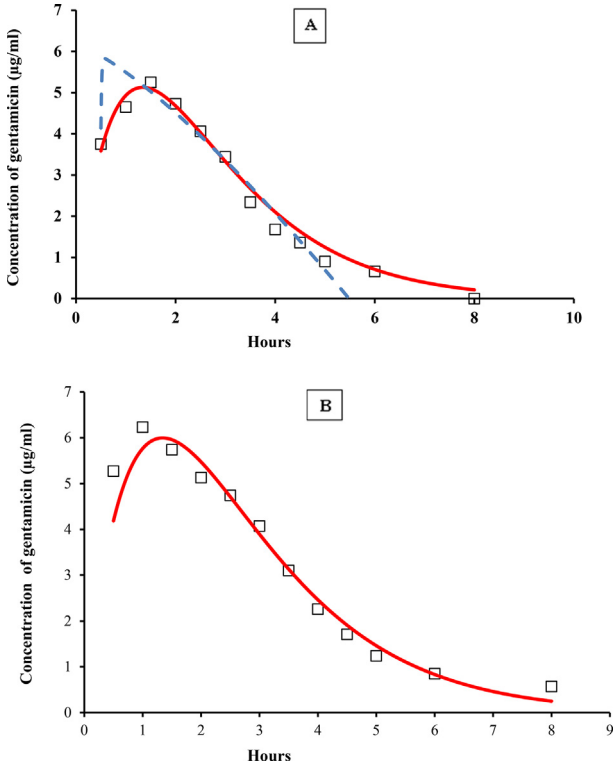

Fig. 9. Mathematical modeling of *in vivo* pharmacokinetic profile of gentamicin in blood plasma. A) P1 (PLGA alone) and B) P2 (CβG/PLGA = 0.5:99.5 %). Solid line - exponential drug release, dotted line – Korsmeyer - Peppas model for drug release.

4. Conclusions

The current study describes the advantages of blending the biopolymer CβG with synthetic PLGA. A mathematical model was developed to predict the degradation of the polymer as a function of time and the drug release *in vitro*. Initial burst release followed by sustained release was observed in all the blends *in vitro*, and the drug released from the nanoparticles was active against *E. coli*. A double exponential model was developed to successfully predict the gentamicin concentration as a function of time in the blood. Prolonged drug release (8 h) was observed

with blend *in vivo*. To conclude, glucan blended polymer could be used as a carrier for delivery of toxic drugs to achieve therapeutic index similar to the pure drug with reduced toxicity.

Declarations

Author contribution statement

Geetha Venkatachalam: Conceived and designed the experiments; Performed the experiments; Wrote the paper.

Nandakumar Venkatesan: Analyzed and interpreted the data; Contributed reagents, materials, analysis tools or data.

Ganesan Suresh: Contributed reagents, materials, analysis tools or data.

Mukesh Doble: Analyzed and interpreted the data.

Funding statement

This research did not receive any specific grant from funding agencies in the public, commercial, or not-for-profit sectors.

Competing interest statement

The authors declare no conflict of interest.

Additional information

Supplementary content related to this article has been published online at https://doi.org/10.1016/j.heliyon.2019.e02289.

Acknowledgements

The authors thank Mrs. Divyaa Srinivasan for her help in polymer blending process. The authors also thank the Sophisticated Analytical Instrument Facility (SAIF), IIT-Madras for analytical help.

References

[1] M.W. Breedveld, K.J. Miller, Cyclic beta-glucans of members of the family Rhizobiaceae, Microbiol. Rev. 58 (2) (1994) 145–161.
[2] J. Piao, A. Jang, Y. Choi, M.N. Tahir, Y. Kim, S. Park, E. Cho, S. Jung, Solubility enhancement of α-naphthoflavone by synthesized hydroxypropyl cyclic-(1→ 2)-β-d-glucans (cyclosophoroases), Carbohydr. Polym. 101 (2014) 733–740.
[3] A.G. Matthysse, Exopolysaccharides of *Agrobacterium tumefaciens*, Agrobact. Biol.: From Basic Science to Biotechnology 418 (2018) 111–141.
[4] G. Venkatachalam, S. Gummadi, M. Doble, Cyclic β-Glucans from Microorganisms, Production, Properties and Applications, Springer science & Business Media, 2012.
[5] G. Venkatachalam, D. Srinivasan, M. Doble, Cyclic β-(1, 2)-glucan production by *Rhizobium meliloti* MTCC 3402, Process Biochem. 48 (12) (2013) 1848–1854.
[6] S.-H. Lee, E. Cho, S.-H. Jung, Periplasmic glucans isolated from Proteobacteria, BMB Rep. 42 (12) (2009) 769–775.
[7] Y. Hu, H. Kim, V.V. Shinde, D. Jeong, Y. Choi, E. Cho, S. Jung, Carboxymethyl cyclosophoraoses as a flexible ph-responsive solubilizer for pindolol, Carbohydr. Polym. 175 (2017) 493–501.
[8] K. Koizumi, Y. Okada, S. Horiyama, T. Utamura, T. Higashiura, M. Ikeda, Preparation of cyclosophoraose-A and its complex-forming ability, J. Inclusion Phenom. 2 (3-4) (1984) 891–899.
[9] N.S.V. Kambhampati, S. Kar, S.S.K. Pinnepalli, J. Chelli, M. Doble, Microbial cyclic β-(1→ 3),(1→ 6)-Glucans as potential drug carriers: interaction studies between cyclic β-glucans isolated from *Bradyrhizobium japonicum* and betulinic acid, Spectrochim. Acta A Mol. Biomol. Spectrosc. 203 (2018) 494–500.
[10] H. Kim, K. Jeong, S. Lee, S. Jung, Molecular dynamics simulation of cyclosophoroheptadecaose (Cys-A), J. Comput. Aided Mol. Des. 16 (8-9) (2002) 601–610.
[11] Y.-H. Choi, C.-H. Yang, H.-W. Kim, S. Jung, Molecular dynamics simulations of cyclohenicosakis-[(1→ 2)-β-d-gluco-henicosapyranosyl], a cyclic (1→ 2)-β-d-glucan (a 'cyclosophoraose') of DP 21, Carbohydr. Res. 326 (3) (2000) 227–234.
[12] M. Mimura, S. Kitamura, S. Gotoh, K. Takeo, H. Urakawa, K. Kajiwara, Conformation of cyclic and linear (1→ 2)-β-D-glucans in aqueous solution, Carbohydr. Res. 289 (1996) 25–37.
[13] I. André, K. Mazeau, F.R. Taravel, I. Tvaroska, Conformation and dynamics of a cyclic (1→ 2)-β-d-glucan, Int. J. Biol. Macromol. 17 (3-4) (1995) 189–198.
[14] G. Venkatachalam, V. Nandakumar, G. Suresh, M. Doble, Characterization and applications of cyclic β-(1, 2)-glucan produced from R. meliloti, RSC Adv. 4 (22) (2014) 11393–11399.
[15] H.K. Makadia, S.J. Siegel, Poly lactic-co-glycolic acid (PLGA) as biodegradable controlled drug delivery carrier, Polymers 3 (3) (2011) 1377–1397.
[16] D.T. Birnbaum, J.D. Kosmala, D.B. Henthorn, L. Brannon-Peppas, Controlled release of β-estradiol from PLAGA microparticles: the effect of organic phase solvent on encapsulation and release, J. Control. Release 65 (3) (2000) 375–387.
[17] K.E. Lee, B.K. Kim, S.H. Yuk, Biodegradable polymeric nanospheres formed by temperature-induced phase transition in a mixture of poly (lactide-co-glycolide) and poly (ethylene oxide)– poly (propylene oxide)– poly (ethylene oxide) triblock copolymer, Biomacromolecules 3 (5) (2002) 1115–1119.
[18] P. Liu, H. Yu, Y. Sun, M. Zhu, Y. Duan, A mPEG-PLGA-b-PLL copolymer carrier for adriamycin and siRNA delivery, Biomaterials 33 (17) (2012) 4403–4412.
[19] P.J. Kennedy, F. Sousa, D. Ferreira, C. Pereira, M. Nestor, C. Oliveira, P.L. Granja, B. Sarmento, Fab-conjugated PLGA nanoparticles effectively target cancer cells expressing human CD44v6, Acta Biomater. 81 (2018) 208–218.
[20] V. Nandakumar, V. Geetha, S. Chittaranjan, M. Doble, High glycolic poly (DL lactic co glycolic acid) nanoparticles for controlled release of meropenem, Biomed. Pharmacother. 67 (5) (2013) 431–436.
[21] J.U. Menon, S. Kona, A.S. Wadajkar, F. Desai, A. Vadla, K.T. Nguyen, Effects of surfactants on the properties of PLGA nanoparticles, J. Biomed. Mater. Res. A 100 (8) (2012) 1998–2005.
[22] V. Nandakumar, G. Suresh, S. Chittaranjan, M. Doble, Synthesis and characterization of hydrophilic high glycolic acid–poly (dl-Lactic-co-Glycolic acid)/ polycaprolactam/polyvinyl alcohol blends and their biomedical application as a ureteral material, Ind. Eng. Chem. Res. 52 (2) (2012) 751–760.
[23] Z. Xu, W. Gu, J. Huang, H. Sui, Z. Zhou, Y. Yang, Z. Yan, Y. Li, In vitro and in vivo evaluation of actively targetable nanoparticles for paclitaxel delivery, Int. J. Pharma. 288 (2) (2005) 361–368.
[24] L. Mu, S. Feng, A novel controlled release formulation for the anticancer drug paclitaxel (Taxol®): PLGA nanoparticles containing vitamin E TPGS, J. Control. Release 86 (1) (2003) 33–48.
[25] R. De La Fuente, N. Sonawane, D. Arumainayagam, A. Verkman, Small molecules with antimicrobial activity against *E. coli* and *P. aeruginosa* identified by high-throughput screening, Br. J. Pharmacol. 149 (5) (2006) 551–559.
[26] P.K. Prabhakar, S. Raj, P. Anuradha, S.N. Sawant, M. Doble, Biocompatibility studies on polyaniline and polyaniline–silver nanoparticle coated polyurethane composite, Colloids Surfaces B Biointerfaces 86 (1) (2011) 146–153.
[27] R.K. Averineni, G.V. Shavi, A.K. Gurram, P.B. Deshpande, K. Arumugam, N. Maliyakkal, S.R. Meka, U. Nayanabhirama, PLGA 50: 50 nanoparticles of paclitaxel: development, in vitro anti-tumor activity in BT-549 cells and in vivo evaluation, Bull. Mater. Sci. 35 (3) (2012) 319–326.
[28] J.P. Anhalt, S.D. Brown, High-performance liquid-chromatographic assay of aminoglycoside antibiotics in serum, Clin. Chem. 24 (11) (1978) 1940–1947.
[29] T. Phromsopha, Y. Baimark, Chitosan microparticles prepared by the water-in-oil emulsion solvent diffusion method for drug delivery, Biotechnology 9 (1) (2010) 61–66.
[30] Y. Ling, Y. Huang, Preparation and Release Efficiency of Poly (Lactic-co-glycolic) Acid Nanoparticles for Drug Loaded Paclitaxel, 7th Asian-Pacific Conference on Medical and Biological Engineering, Springer, 2008, pp. 514–517.
[31] S. Ravi, K. Peh, Y. Darwis, B.K. Murthy, T.R.R. Singh, C. Mallikarjun, Development and characterization of polymeric microspheres for controlled release protein loaded drug delivery system, Indian J. Pharm. Sci. 70 (3) (2008) 303.
[32] R.W. Korsmeyer, R. Gurny, E. Doelker, P. Buri, N.A. Peppas, Mechanisms of solute release from porous hydrophilic polymers, Int. J. Pharma. 15 (1) (1983) 25–35.
[33] M.R. Virto, B. Elorza, S. Torrado, M.d.L.A. Elorza, G. Frutos, Improvement of gentamicin poly (D, L-lactic-co-glycolic acid) microspheres for treatment of osteomyelitis induced by orthopedic procedures, Biomaterials 28 (5) (2007) 877–885.
[34] A. Kumari, S.K. Yadav, S.C. Yadav, Biodegradable polymeric nanoparticles based drug delivery systems, Colloids Surfaces B Biointerfaces 75 (1) (2010) 1–18.
[35] Y. Parajó, I. d'Angelo, A. Horváth, T. Vantus, K. György, A. Welle, M. Garcia-Fuentes, M.J. Alonso, PLGA: poloxamer blend micro-and nanoparticles as controlled release systems for synthetic proangiogenic factors, Eur. J. Pharm. Sci. 41 (5) (2010) 644–649.
[36] A. des Rieux, V. Pourcelle, P.D. Cani, J. Marchand-Brynaert, V. Préat, Targeted nanoparticles with novel non-peptidic ligands for oral delivery, Adv. Drug Deliv. Rev. 65 (6) (2013) 833–844.
[37] N. Butoescu, O. Jordan, A. Petri-Fink, H. Hofmann, E. Doelker, Co-encapsulation of dexamethasone 21-acetate and SPIONs into biodegradable polymeric microparticles designed for intra-articular delivery, J. Microencapsul. 25 (5) (2008) 339–350.
[38] N. Butoescu, O. Jordan, P. Burdet, P. Stadelmann, A. Petri-Fink, H. Hofmann, E. Doelker, Dexamethasone-containing biodegradable superparamagnetic microparticles for intra-articular administration: physicochemical and magnetic properties, in vitro and in vivo drug release, Eur. J. Pharm. Biopharm. 72 (3) (2009) 529–538.
[39] S. Manoochehri, B. Darvishi, G. Kamalinia, M. Amini, M. Fallah, S.N. Ostad, F. Atyabi, R. Dinarvand, Surface modification of PLGA nanoparticles via human serum albumin conjugation for controlled delivery of docetaxel, Daru 21 (1) (2013) 58.
[40] C. Kwon, Y. Choi, D. Jeong, J.G. Kim, J.M. Choi, S. Chun, S. Park, S. Jung, Inclusion complexation of naproxen with cyclosophoraoses and succinylated cyclosophoraoses in different pH environments, J. Inclusion Phenom. Macrocycl. Chem. 74 (1-4) (2012) 325–333.

[41] L.Z. Benet, D. Kroetz, L. Sheiner, J. Hardman, L. Limbird, Pharmacokinetics: the Dynamics of Drug Absorption, Distribution, Metabolism, and Elimination, Goodman and Gilman's the Pharmacological Basis of Therapeutics, 1996, pp. 3–27.
[42] S.Y. Lee, J.X. Cheng, Clearance of nanoparticles during circulation, Pharm. Sci. Encycl.: Drug Disc. Develop. Manufact. (2010) 1–32.
[43] J. Morin, G. Viotte, A. Vandewalle, F. Van Hoof, P. Tulkens, J. Fillastre, Gentamicin-induced nephrotoxicity: a cell biology approach, Kidney Int. 18 (5) (1980) 583–590.
[44] G. Evans, A Handbook of Bioanalysis and Drug Metabolism, CRC press, 2004.